Electronic Supplementary Material (ESI) for Nanoscale.

Supporting Information

SiO_2/Ta_2O_5 heterojunction ECM memristor: Physical nature of their low voltage operation with high stability and uniformity

Xiangyu Guo, Qi Wang, Xiaowei Lv, Huiyong Yang, Kai Sun, Dongliang Yang, Haitao Zhang, Tsuyoshi Hasegawa and Deyan He*

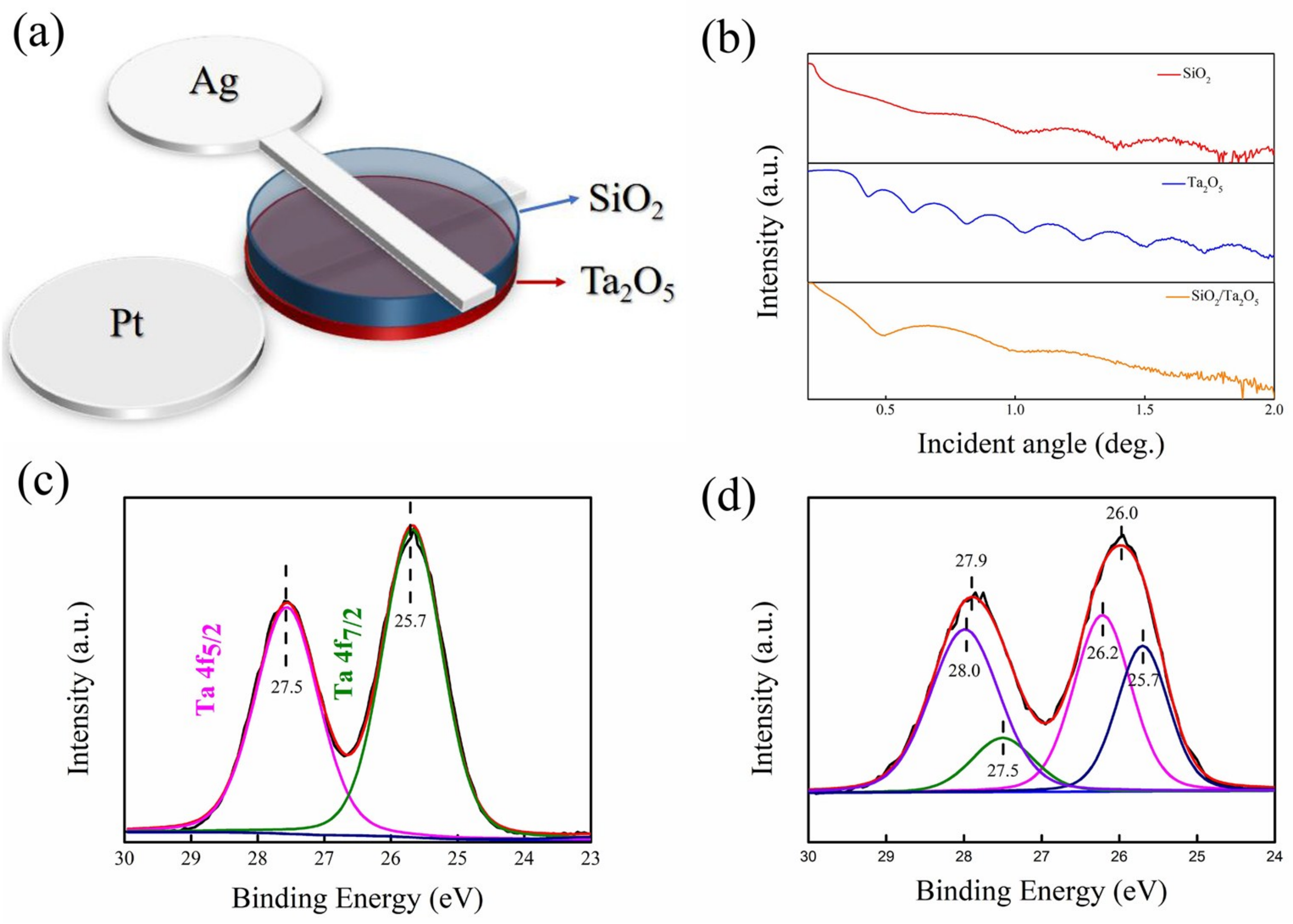

Figure S1. a) Cross-bar structure diagram. b) X-ray reflective measurement. X-ray photoelectron spectra of Ta 4f core-line spectra taken for c) SiO_2 (5nm) and d) Ta_2O_5/SiO_2.

Figure S1a shows the cross-bar structure diagram of the Ag/SiO_2/Ta_2O_5/Pt devices. The same structure is used for the Ag/SiO_2(7nm)/Pt single layer devices, the Ag/Ta_2O_5(15nm)/Pt single layer devices and the Ag/ Ta_2O_5(1.5nm)/ SiO_2(5nm)/Pt devices. Figure S1b shows the result of X-ray reflective (X'Pert MRD), the density of Ta_2O_5 is 7.65 g/cm^3 and the density of SiO_2 is 2.39 g/cm^3. In Figure S1c-d, the Ta 4f peak position was increased by about 0.3 eV due to the formation of a partial O-Ta-Si bond at the interface.

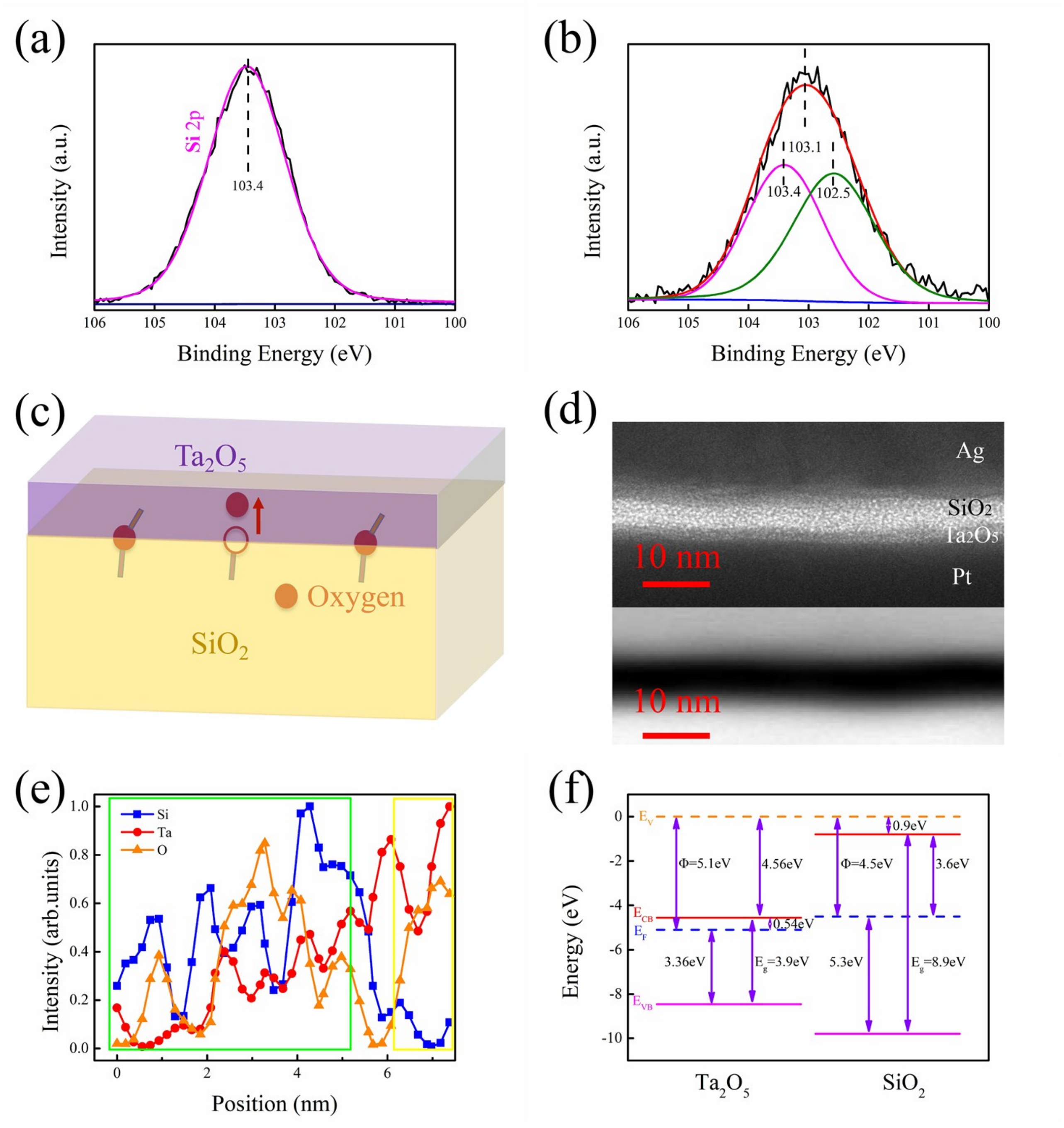

Figure S2. X-ray photoelectron spectra of Si 2p core-line taken for a) SiO_2 (5nm) and b) Ta_2O_5 (1.5nm)/SiO_2 (5nm). c) Schematic of the defect formation at the interface of Ta_2O_5/SiO_2. A part of oxygen atoms in SiO_2 move into the Ta_2O_5. d) The dark-field and bright-field cross-sectional TEM images of Ag/SiO_2 (5nm)/Ta_2O_5 (1.5nm)/Pt device. e) The cross-sectional EDS depth profile of Ag/SiO_2/Ta_2O_5/Pt device. f) Schematic of the band alignment at the Ta_2O_5-SiO_2 interface.

Figures S2a and b show the Si 2p core-line XPS spectra of SiO_2 before and after the formation of 1.5nm-thick Ta_2O_5 layer on it by RF magnetron sputtering. The energy levels were precisely calibrated by the peak of C 1s with a standard binding energy of 284.6 eV. Then, the chemical component of the samples was analysed. In Figure S2a, Si 2p spectra that has a peak at 103.4 eV suggests single Si oxidation state of Si^{4+}, which has a binding energy of 103.5 eV, as previously reported.[1] On the other hand, the peak in Figure S2b for Ta_2O_5/SiO_2 can be fitted as two doublets, in which the additional component (peak-II) of Si^{3+} is observed at a lower binding energy of 102.5 eV. It has been reported that difference in areal density of oxygen atoms at an interface of high-k materials and SiO_2 is considered as an intrinsic origin of the dipole formation.[2, 3] Our XPS spectra indicates that oxygen at the interface moves from the SiO_2 layer to the Ta_2O_5 layer, resulting in the defect formation at the interface as shown in Figure S2c. Figure S2d shows the dark-field and bright-field TEM images of a cross-section. Figure S2e shows EDS depth profile of Si, Ta and O in SiO_2/Ta_2O_5 double layer. Although it does not show the exact ratio of elements in the thin film, we can see the overview of the elements' distribution.[4] The green box corresponds to the SiO_2 layer, and the yellow box corresponds to the Ta_2O_5 layer. It is obvious that the oxygen density decreases at the interface, especially in the SiO_2 layer side. This result coincides with the XPS result. Figure S2f shows schematic of the band alignment at the Ta_2O_5/SiO_2 interface, calculated from UPS and U-V vis absorption spectrum shown in Figure S3, Supporting Information.

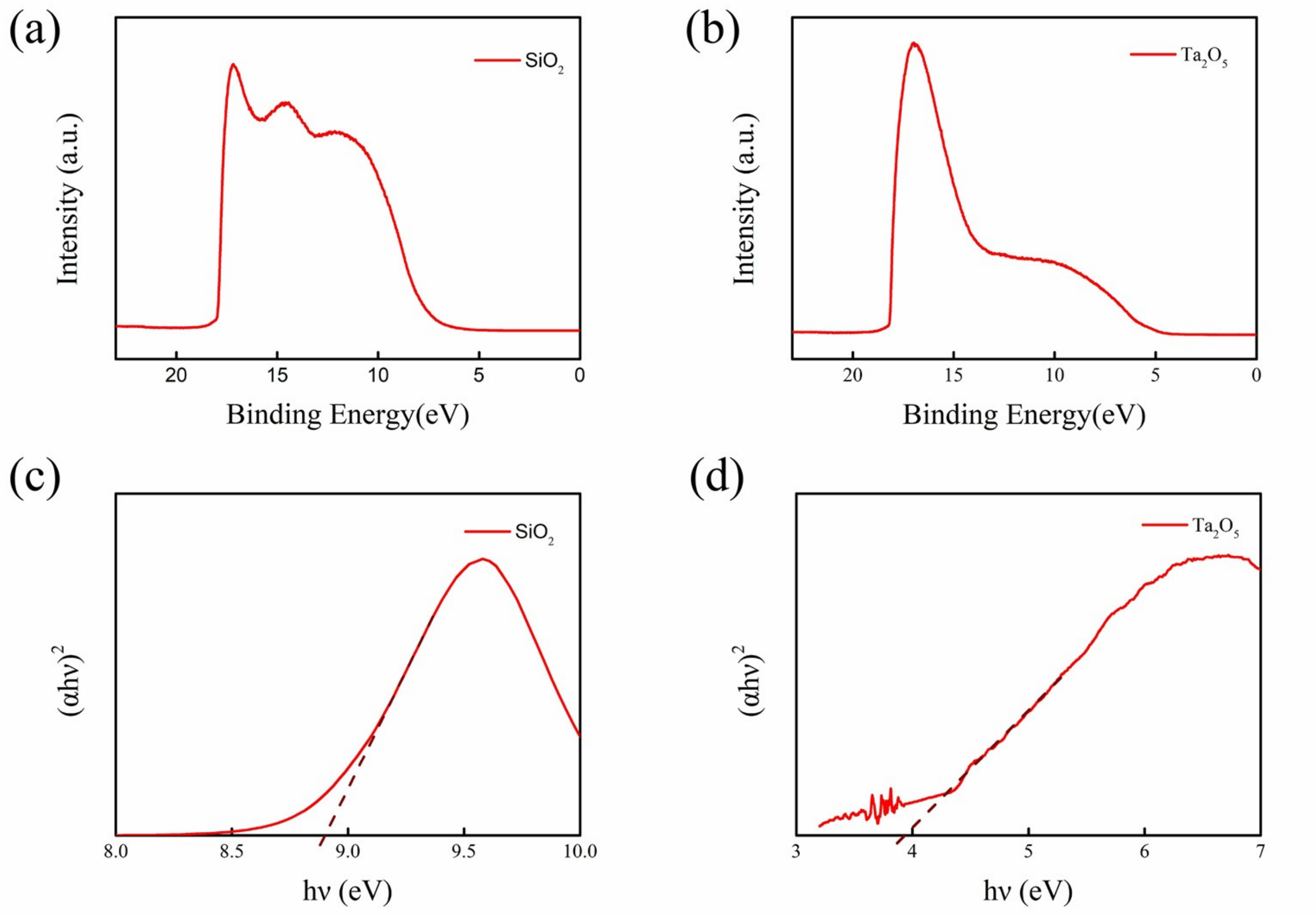

Figure S3. The UPS spectra of a) SiO_2 film and b) Ta_2O_5 film. The $(\alpha h\nu)^2$-hν curves of c) SiO_2 and d) Ta_2O_5 films.

The work function of these materials was determined from UPS spectra using the expression Work function (Φ) = hʋ - ($E_{cut - off} - E_F$), hʋ is the energy of the He-I source (21.2 eV) as shown in Figure S3a-b. In Figure S3c-d, the study on the UV–vis absorption spectrum and the transformed curves $(\alpha h\nu)^2$-hν of SiO_2 film and Ta_2O_5 film was conduct. The band-gap energy (E_g) of SiO_2 was about 8.9 eV, and the band-gap energy (E_g) of Ta_2O_5 was about 3.9 eV.

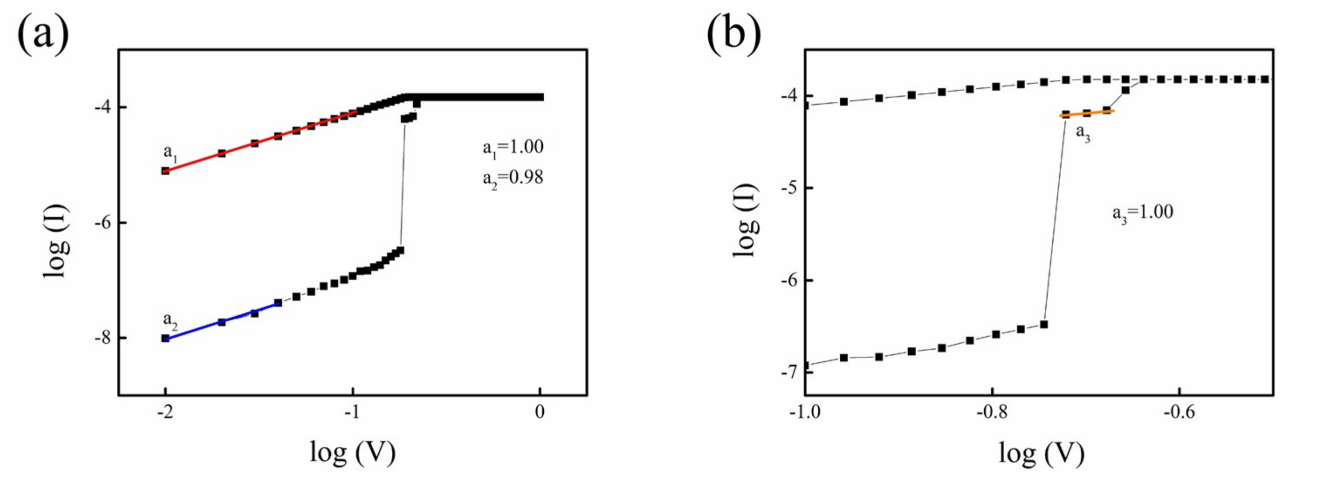

Figure S4. Log(I)-log(V) plot fitting for I-V characteristics of the Ag/SiO_2/Ta_2O_5/Pt device.

In Figure S4, Figure b is a partial enlargement of Figure a. a1, a2 and a3 indicating ohmic conduction with a slope of roughly 1. It indicate that complete conductive filaments have been formed, when the voltage is abrupt to about 60uA. As the voltage increases, the new conductive filament are formed and exhibit a multi-level state.

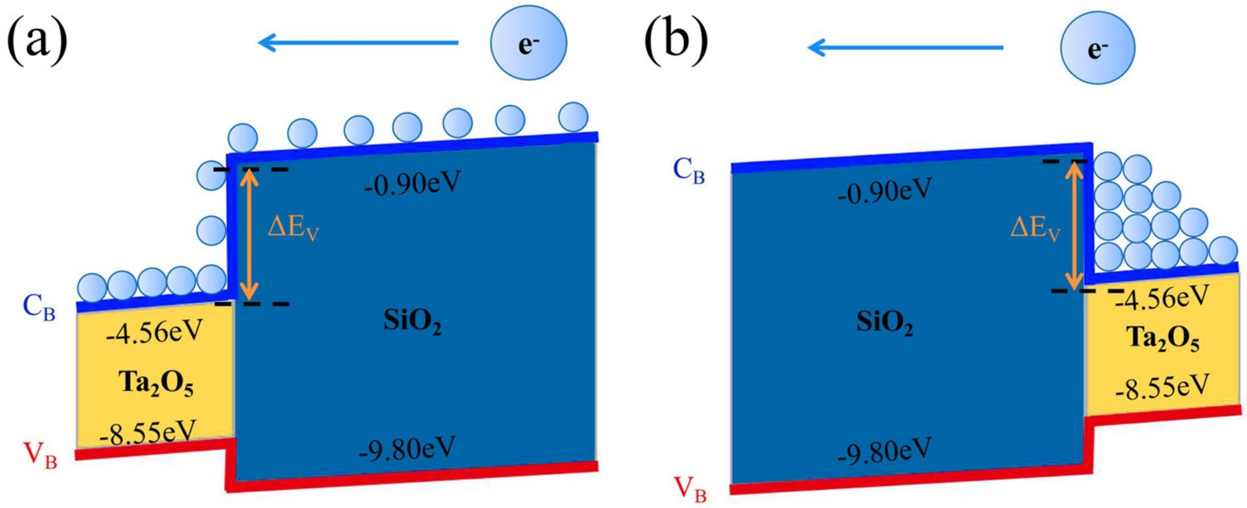

Figure S5. Band diagram at the interface of Ag/Ta_2O_5/SiO_2/Pt, where electrons could smoothly pass the interface. d) In the case of Ag/SiO_2/Ta_2O_5/Pt, electrons would be trapped in the interface.

Band diagrams of Ag/Ta_2O_5/SiO_2/Pt and Ag/SiO_2/Ta_2O_5/Pt when applied positive bias to Ag electrode for forming processes are shown in Figures S5a and b, respectively. In the case of Ag/Ta_2O_5/SiO_2/Pt, electrons easily go through the Ta_2O_5/SiO_2 interface. Therefore, CFs start to grow near the interface because Ag ions also easily reach the interface though the Ta_2O_5 layer. However, it is hard to control the growth direction of CFs afterwards. As a result, we do not know in which oxide layer a diameter of a CF is thinner. CFs may dissolve sometimes in the Ta_2O_5 layer, but sometimes in the SiO_2 layer. This uncontrollability on the thinner part of CFs should result in the larger range of the switching voltage, although the half of the set/reset voltages, i.e., 25%-75%, distributes in the narrow ranges.

On the other hand, some electrons are trapped at the interface between SiO_2 and Ta_2O_5 layer in the case of Ag/SiO_2/Ta_2O_5/Pt, as shown in Figure S5b. Since the Ag ion's mobility is low in SiO_2, Ag ions will be nucleated near the Ag electrode inside SiO_2 and the repeated nucleation and growth leads to the filament shape as conical. After reaching the interface, Ag filament growth becomes more easy because of the high mobility of Ag ions in Ta_2O_5 and larger number of electrons in the conduction band (C_B), making the obconical shape of Ag filament. This obconical shape of CFs causes the dissolution always in the ultra-thin Ta_2O_5 layer. Since CFs in a SiO_2 layer remain after each reset process, electric field effectively concentrates on the remaining CFs where the re-formation of CFs occurs, not in the other places. This is the reason why the Ag/SiO_2/Ta_2O_5/Pt devices show highly uniform switching with low switching bias.

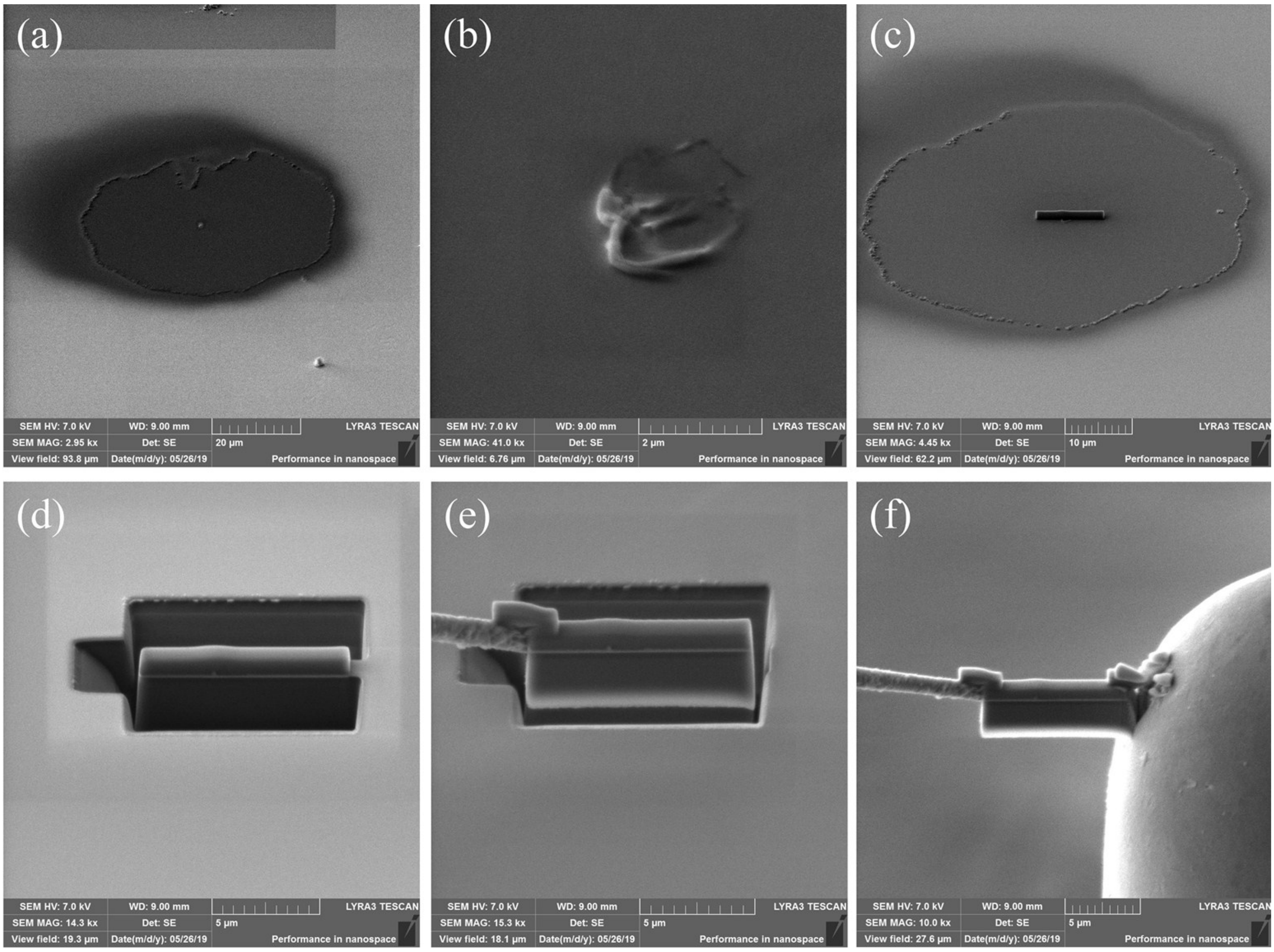

Figure S6. a-f) Top-view SEM image of the ex-situ TEM sample production process.

First, we measured the Ag/SiO_2/Ta_2O_5/Pt device with the repeated switching cycle for 50 times. After the measurement, the filament could be formed around the contact area of the probe with the top electrode. Figure S6b shows the enlarged image of the contact area, which causes a slight pit left after the measurement process. We prepared the lamellae sample on the pit as shown in Figure S6c. The fabricated TEM sample provided the observation area with the dimensions of 7μm×1μm as shown in Figure S6d. The sample was thinned and the thickness after thinning was about 100 nm, which is shown in Figure S6e-f..

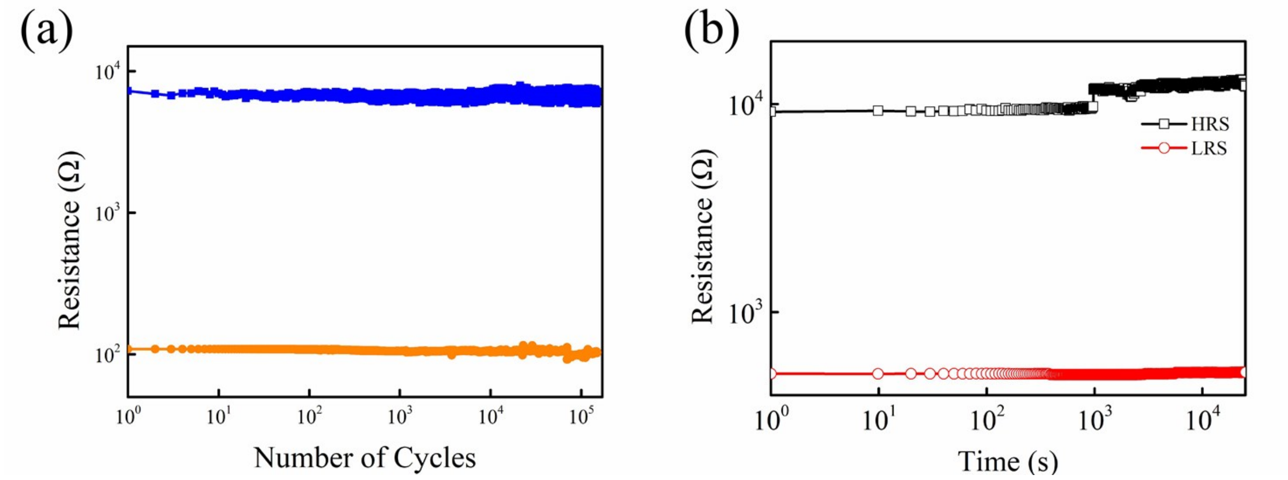

Figure S7. a) Pulse endurance test under 1 ms pulse of the Ag/SiO_2/Ta_2O_5/Pt devices. b) The HRS/LRS retention time.

In FigureS7, we used voltage pulses (fixed width of 1 ms) to test the endurance of the Ag/SiO_2/Ta_2O_5/Pt devices. Switching was carried out by 1.2V, 1 ms for set and −1V , 1 ms voltage pulses for reset. The reading voltage is 10mV, 100ms. The pulse power used in the test was keithley2636B. The HRS/LRS retention time as shown in Figure S7b, the reading voltage is 5mV.

1 D. Xing, H. Zeng, W. Zhang and W. Zhang, *IOP Conf. Ser. Mater. Sci. Eng.* **2019**, 490, 022079.

2 A. Thøgersen, J. H. Selj and E. S. Marstein, *J. Electrochem. Soc.* **2012**, 159, D276.

3 K. Kita and A. Toriumi, *Appl. Phys. Lett.* **2009**, 94, 132902.

4 Z. Fang, H. Y. Yu, X. Li, N. Singh, G. Q. Lo and D. L. Kwong, *IEEE Electron Device Lett.* **2011**, 32, 566.